Giant rotary power of a fishnet-like metamaterial

S.X. Wang, F. Garet, Eric Lheurette, M. Astic, J.L. Coutaz, D. Lippens

APL Materials

Giant rotary power of a fishnet-like metamaterial

Cite as: APL Mater. 1, 032116 (2013); https://doi.org/10.1063/1.4821627
Submitted: 21 February 2013 • Accepted: 17 June 2013 • Published Online: 19 September 2013

Shengxiang Wang, Frédéric Garet, Éric Lheurette, et al.

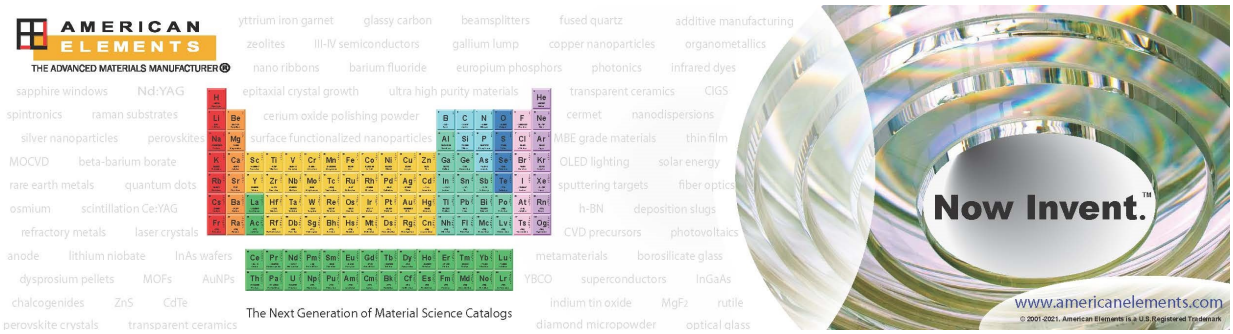

Giant rotary power of a fishnet-like metamaterial

Shengxiang Wang,[1,2] Frédéric Garet,[3] Éric Lheurette,[1,a] Magali Astic,[3] Jean-Louis Coutaz,[3] and Didier Lippens[1]

[1]*Institut d'Électronique de Microélectronique et Nanotechnologies, Université de Lille 1, Avenue Poincaré BP 60069, 59652 Villeneuve d'Ascq Cedex, France*
[2]*School of Electronics and Electrical Engineering, Wuhan Textile University, Hubei, Wuhan, People's Republic of China*
[3]*Laboratoire IMEP-LAHC, Université de Savoie, 73376 Le Bourget du Lac Cedex, France*

(Received 21 February 2013; accepted 17 June 2013; published online 19 September 2013)

We show experimentally and numerically that cholesteric-type metal-dielectric structures, made of twisted sub-wavelength hole elliptical–shaped arrays, exhibit strong optical activity and circular dichroism. The experimental demonstration is carried out with terahertz time-domain spectroscopy measurements on a three layered structure operating around 0.5 THz, leading to a rotary power as high as 1000°/wavelength. The contribution of the chirality factor (κ), permittivity (ε), and permeability (μ) is discussed after the retrieval of effective parameters from the complex scattering ones.
[http://dx.doi.org/10.1063/1.4821627]

Conventional Negative Index Metamaterials (NIM) are fabricated from periodically arranged artificial structures,[1] which exhibit effective negative permittivity (ε) and negative permeability (μ). Recently, chiral artificial structures, made of unit cells that are non-superimposable on their mirror image, have been independently suggested as an alternative route to negative refraction.[2,3] In 2003, Tretyakov *et al.* first discussed this possibility by means of a metamaterial including chiral motifs such as helical wires.[2] Swiss-roll structures, wounded in a helical manner, have also been proposed in 2004 as a possible solution to achieve negative refractive index. Both approaches do not require simultaneously negative permittivity and permeability in the same frequency range as for conventional NIM. This concept has been first experimentally demonstrated in 2009 at microwaves by Zheludev's group using a 3D-chiral metamaterial based on stacked layers of mutually twisted rosettes.[4] This work pointed out the role of antisymmetric and symmetric resonances modes between two superimposed patterns for the negative refraction of right- and left-handed circularly polarized waves, respectively. The same year, experimental negative refraction at THz frequencies, by means of chirality, has also been published by Zhang and co-workers.[5] In this case, the chirality was achieved by an orthogonal arrangement of parallel strips interconnected by airbridges.

Following the multi-layer arrangement, various patterns have been extensively studied like, for instance, crossed wires[6] and U-shaped basic cells.[7] These studies on chiral metamaterials also revealed outstanding potentials in terms of rotary power. Indeed, giant rotary power (several orders of magnitude stronger than a girotropic quartz crystal) was demonstrated experimentally and numerically at the microwave wavelengths, in the articles cited previously notably.[4,6] Optical activity and circular dichroism were also observed in the optical regime on the basis of nanoscaled bilayered chiral structures.[8–10] Back in 2001, strong rotary power had already been predicted by Zheludev and co-workers from a structure involving two layers of mutually twisted strips.[11] From the experimental side, giant girotropy by means of bilayered metallic twisted rosettes has been observed at

[a]Author to whom correspondence should be addressed. Electronic mail: eric.lheurette@iemn.univ-lille1.fr

microwaves in 2006[12] and at infrared in 2007.[13] Besides, strong polarization rotation has also been demonstrated from a metallic plate perforated by chiral subwavelength apertures and the role of the chirality of the patterns in the polarization conversion has been pointed out.[14]

In the present paper, we show pronounced chirality properties of a twisted layered fishnet-like structure composed of sub-wavelength holes arrays. The fabricated devices include elliptical apertures so that the transmissivity is sensitive to polarization (the highest transmission is obtained for an electric field direction along the small axis). The elliptical axis direction is twisted during the stacking of the hole arrays so that the layered periodic arrangement can be compared to the cholesteric one of liquid crystals according to Friedel's nomenclature.[15] This basic scheme, easier to fabricate than non-planar structures, is quite general and could be implemented in principle from microwave to the optical spectrum. Proof of first principle is here demonstrated at the THz frequencies. To this aim, *angle resolved* frequency dependence of the complex scattering parameters of a three-layered slab were measured from 0.4 to 0.6 THz using time-domain spectroscopy (TDS). On the basis of these measurements, the polarization rotation angle θ and the ellipticity angle η are deduced, demonstrating a strong rotary power, defined as the rotation angle of the polarization of the electromagnetic wave between the input and output planes of the twisted metamaterial, around 1000°/wavelength. The frequency dependence of θ and η are subsequently compared with the theoretical values which were calculated by full wave numerical analysis. These calculations permit us to retrieve the effective parameters from the constitutive equations. Finally, the dispersion of these parameters is discussed.

The basic cell of each layer consists in an elliptical aperture etched in a thin metal foil. From our previous experimental and theoretical investigations related to un-twisted fishnets,[16] it was shown that such a metamaterial structure exhibits negative refractive index in a spectral region where ε and μ are simultaneously negative (around 0.5 THz), provided than at least two layers are stacked. Negative refractive index values for this non-chiral structure were assessed, on one hand, by means of Fresnel inversion procedure from the transmission and reflectance measurements[17] and, on the other hand, via direct refraction angle measurements on a wedge-shaped device.[18] Electromagnetic behavior was predicted with the help of full wave numerical simulations. This analysis permitted one to point out the contributions of (i) surface plasmons with a resonant condition on the period of the transverse array and (ii) sub-cut-off propagation through the elliptical apertures. Also, from lumped element circuit approach, a model based on parallel and shunt LC circuits was proposed in order to explain the resonant character of the propagation.[19] In addition, it was shown that the highest transmissivity is achieved for an Elliptical Aspect Ratio ($EAR = a_x/a_y$, where a_x and a_y are the large and small axis of the ellipse) equal to 1.8:1, with the electric field polarization oriented along the small axis. It can be verified that such a criterion is a direct consequence of the matching impedance condition, which requires that the dispersion characteristics of ε and μ are comparable via the equality of the magnetic and electrical plasma frequencies. Under this condition, the metamaterial exhibits a *balanced* Composite Right Left Handed behavior. At the turning frequency between negative and positive values of ε and μ, such an artificial structure can be considered as a *nihil* metamaterial as first discussed in the pioneering work of Tretyakov *et al.*[2]

We target here to introduce some chirality in the electromagnetic behavior through symmetry breaking and by taking benefit of the polarization sensitivity aforementioned. To this aim, elliptical hole, is sequentially rotated by 45° for the consecutive stacked layers, as illustrated in Fig. 1. For the 3-layers structure considered here, this corresponds to an overall rotation of 90°.

Chiral devices were fabricated following the technological procedure implemented for the fabrication of membrane-like *slab* metamaterials.[17] The chiral device is composed of three gold layers, separated by a 26-μm thick BenzoCycloButene (BCB) dielectric layer whose relative permittivity $\varepsilon_r = 2.6$ and loss tangent $tan\ \delta = 10^{-2}$. Metal layers are 400 nm-thick sputtered Au films. The patterning of holes ($a_y = 125\ \mu$m, $EAR = 1.8{:}1$) was achieved by photolithography using *Micro-Chemicals* AZ nLof 2070 negative resist and subsequent lift-off. The periodicities along the small and large axes are both equal to 340 μm. The BCB dielectric layers were deposited by spin coating and subsequent annealed under a nitrogen-controlled atmosphere. Finally, for avoiding the GaAs substrate influence, a deep chemical etch (H_2SO_4: H_2O_2: H_20, 1:8:1) was realized in order to define a membrane. Photograph of the free-standing metamaterial is displayed in Fig. 1(a).

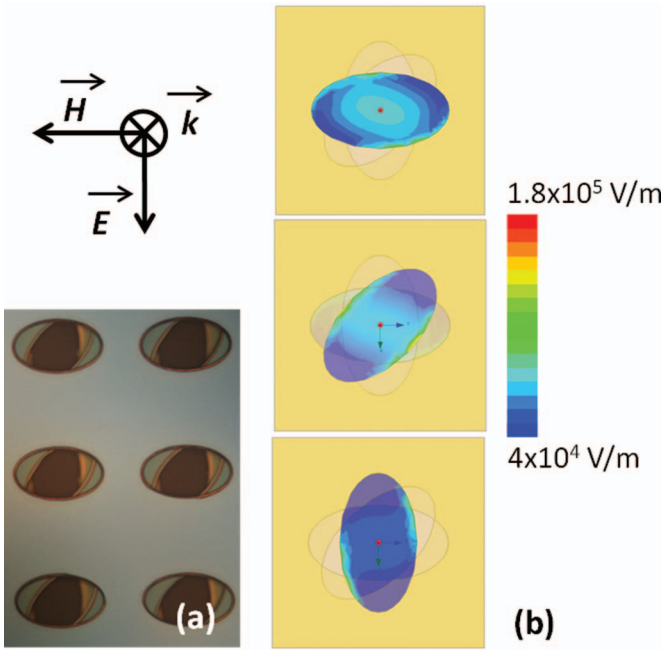

FIG. 1. (a) Microscope view showing the subsequent twisted apertures. (b) Maps of the electric field in the three micro-structured metal layers at $f = 0.468$ THz.

The assessment of chiral properties can be performed via the chirality factor κ that couples the electric/magnetic inductions ($\vec{D}/\vec{B}$) to the electric and magnetic fields ($\vec{E}/\vec{H}$) via the effective parameters (μ and ε) according to the following constitutive equations,[4] where ε_0, μ_0, and c_0 are the vacuum permittivity and permeability and light velocity, respectively,

$$\begin{pmatrix} \vec{D} \\ \vec{B} \end{pmatrix} = \begin{pmatrix} \varepsilon_0\varepsilon & i\kappa/c_0 \\ -i\kappa/c_0 & \mu_0\mu \end{pmatrix} \begin{pmatrix} \vec{E} \\ \vec{H} \end{pmatrix}, \tag{1}$$

$$\kappa = \frac{n_+ - n_-}{2}, \quad n = \frac{n_+ + n_-}{2}, \quad \mu = \frac{z\,(n_+ + n_-)}{2}, \quad \varepsilon = \frac{n_+ + n_-}{2z}. \tag{2}$$

In Eqs. (2), n_+ and n_- are the refractive index of the Right- and Left-handed Circularly Polarized wave (RCP, +) and (LCP, −), respectively, whereas z is the reduced impedance $z = Z/Z_0$with respect to the impedance of vaccum ($Z_0 = 377\ \Omega$). n_+, n_-, and z are related to the reflectance R and transmittances T_+ and T_-, of the RCP and LCP waves, respectively,

$$n_\pm = \frac{i}{k_0 d} \ln\left[\frac{1}{T_\pm}\left(1 - \frac{z-1}{z+1}\right) R\right] = \sqrt{\varepsilon\mu} \pm \kappa, \tag{3}$$

$$z = \sqrt{\frac{(1+R)^2 - T_+T_-}{(1-R)^2 - T_+T_-}}. \tag{4}$$

The transmission coefficient of *circularly* polarized waves (T_+ and T_-) can be related to the four *linear* transmission coefficients $T_{i,j}$ where i or $j = x,y$, by the following equations:[4]

$$\begin{aligned} T_+ &= T_{xx} + T_{yy} + i(T_{xy} - T_{yx}) \\ T_- &= T_{xx} + T_{yy} - i(T_{xy} - T_{yx}), \end{aligned} \tag{5}$$

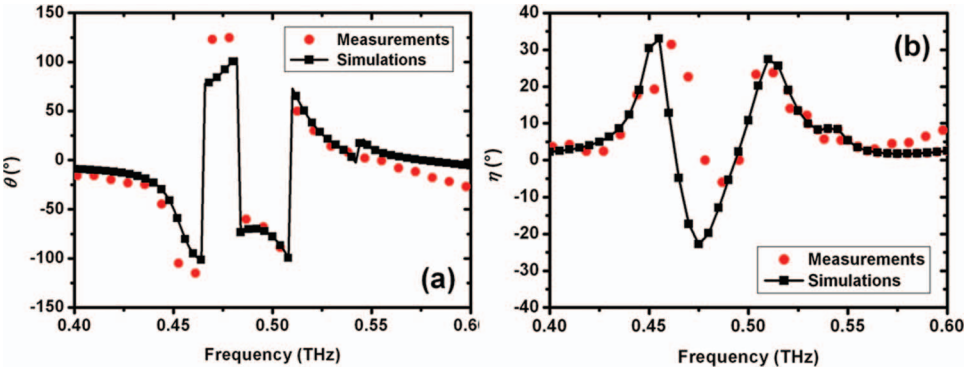

FIG. 2. Frequency dependence of the (a) polarization angle (θ) and (b) ellipticity angle (η).

O_x and O_y are the directions along the small and large axes of the input elliptical holes, respectively. Finally, the polarization rotation angle θ and the ellipticity angle η are defined as

$$\theta = \frac{1}{2}\left[\arg(T_+) - \arg(T_-)\right], \quad \eta = \frac{1}{2}\sin^{-1}\left(\frac{|T_+|^2 - |T_-|^2}{|T_+|^2 + |T_-|^2}\right). \tag{6}$$

In practice, the T_{ij}'s were calculated numerically by means of the finite element commercial code *Ansoft-HFSS* by applying master and slave boundary conditions to a unit cell. Moreover, a finite value of conductivity ($\sigma = 4.1.10^7$ S/m) was assumed for the gold metal layers by reminding that, at THz frequencies, surface waves properties depend mostly on the structure of the metallic films and are not strongly related to the penetration of electromagnetic energy within the metal.

The frequency dependence of θ and η are reported in Figs. 2(a) and 2(b), respectively. The linear combination of the RCP and LCP waves, which propagate, respectively, with the velocities c/n_+ and c/n_-, exhibits a polarization rotation due to the phase shift in the transmission of the two circularly polarized waves through the chiral metamaterial. Sharp responses which are presumably due to magnetic and electric resonances are also noted at 0.46 and 0.48 THz. According to phase advance or phase delay between the clockwise (T_+) and anti-clockwise (T_-) circularly polarized waves, the rotation angle is positive or negative with maximum value greater than 90°. Resonant features of the propagation mechanisms are evidenced via the 180° phase jumps.

With respect to dichroism linked to the difference in the attenuation of transmission T_+ and T_-, it can be seen from Fig. 2(b) that the ellipticity is maximum around 0.45 THz and 0.51 THz. Contrary to the theoretical analysis which was done on the basis of the linear combination of the projection T_{ij} along the main axes, the experimental analysis was performed by a polarization-angle resolved measurement of the transmission coefficients. For this purpose, the sample is located at the waist of a confocal arrangement in the THz-TDS set up (the beam waist is 2 cm at 0.5 THz, while the Rayleigh length (a few centimeters) exceeds strongly the sample thickness). The polarization-sensitive receiving antenna (in practice, a dipole-like Low Temperature Grown GaAs photoconducting antenna) is fixed on a rotation platform, in such a way the antenna sensitivity direction can rotate around its optical axis. This receiving antenna is excited by a 100 fs laser pulse delivered through an optical fiber that allows the rotation of the antenna without changing the set up adjustment. The polarization rotation angle θ and the axes a and b of the elliptical beam are determined as follows: the sample is placed in the THz beam, such as the small axis of the ellipse, is parallel to the incoming THz beam polarization. Then the incoming and transmitted waveforms are measured for a given orientation ϕ of the receiver azimuth angle by 2° steps. The waveforms are Fourier transformed. One can easily show that, for a given frequency, the ratio S of the transmitted and incident signals obeys the following expression:

$$S \propto \sqrt{a^2\cos^2(\phi - \theta) + b^2\sin^2(\phi - \theta)}. \tag{7}$$

Thus, we plot the experimental values of S versus ϕ for each frequency, and we get a, b, and θ by fitting the experimental data with expressions (6). As the antennas supply or detect a linearly

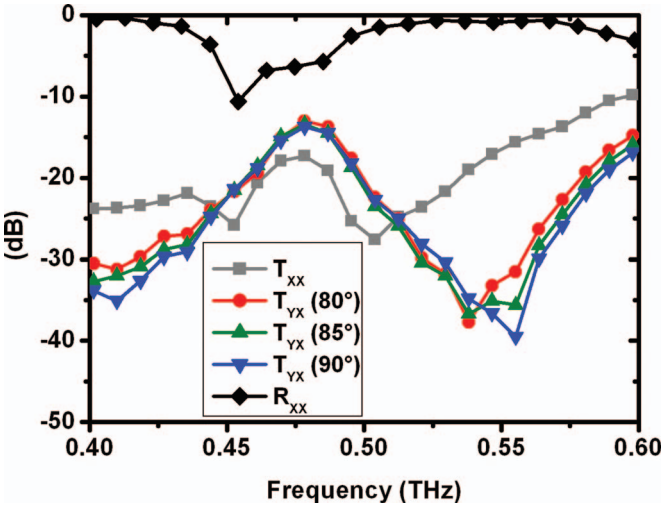

FIG. 3. Frequency dependence of transmission for various angles ϕ ranging between 80° and 90°.

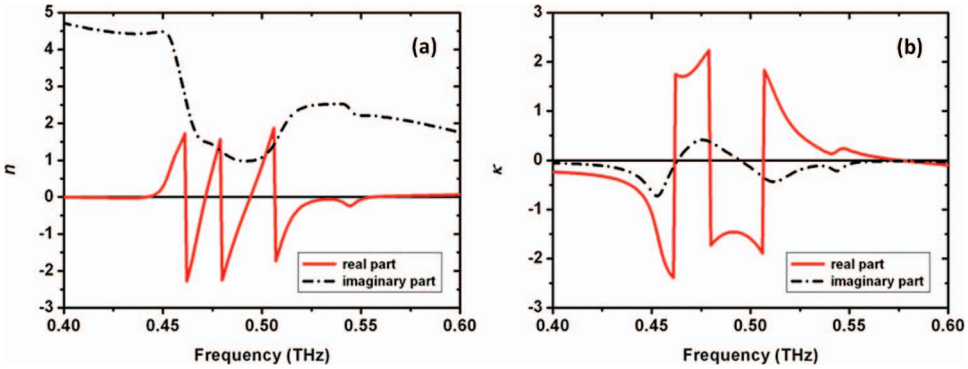

FIG. 4. (a) Complex refractive index n, (b) chirality κ.

polarized THz beam at more than 95%,[20] the direction of the polarization of the transmitted THz beam is measured with a precision of 5°, while its elliptical aspect ratio cannot be determined below 0.1.

Fig. 3 shows the measured frequency dependence of the transmitted wave with the orientation azymuth ϕ of the receiver considered as a parameter. In the frequency window of interest, between 0.4 and 0.6 THz (above higher order propagation modes are expected), the linearly polarized incident wave, whose transmitted angular component is *continuously* recorded here, in contrast to other published works,[4] peaks around 0.48 THz. A maximum is achieved for angle close to 90° as expected owing to the two-fold 45° rotation of the apertures.

For each frequency, the transmitted field component as a function of the angle ϕ was subsequently fitted to the angle dependence of an elliptically polarized wave with the large and small axes of the elliptical beam taken as fitting parameters. The symbols reported in Figs. 2(a) and 2(b) are the result of this fitting procedure. A satisfying agreement is achieved in the comparison of the values of θ and η calculated from Eqs. (6) and those deduced from experimental data.

We further analyzed the various parameters of the constitutive equations (2) by plotting the frequency dependence of the complex parameters n and κ (Fig. 4). The chirality factor reflects the polarization rotation angle. It shows a maximum value around 2 between 0.46 and 0.48 THz. It is important to note that both n_+ and n_- include negative dispersion branches thus leading to saw-like profiles in the evolution of n, showing alternating positive and negative domains. This situation differs from most of the results reported so far on chiral metamaterials. Indeed, our structure is based on a fishnet metamaterial, which behaves as a double negative media due to the superimposed

contributions of a Drude dispersion envelope of the permittivity, and of a resonant feature of the permeability.

In conclusion, a direct experimental evidence of polarization was achieved via angle-resolved measurements of a THz pulse transmitted through a stack of twisted elliptical hole arrays. A strong rotary power around 1000°/wavelength was pointed out experimentally in agreement with full wave analysis and subsequent retrieval of chirality parameter. It is believed that such chiral properties could find useful applications in chemistry, biology, and pharmaceutical for which many molecules are chiral.

[1] D. R. Smith, W. J. Padilla, D. C. Vier *et al.*, "Composite medium with simultaneously negative permeability and permittivity," Phys. Rev. Lett. **84**(18), 4184 (2000).
[2] S. Tretyakov, I. Nefedov, A. Sihvola *et al.*, "Waves and energy in chiral nihility," J. Electromagn. Waves Appl. **17**, 695–706 (2003).
[3] J. B. Pendry, "A chiral route to negative refraction," Science **306**(5700), 1353–1355 (2004).
[4] E. Plum, J. Zhou, J. Dong *et al.*, "Metamaterial with negative index due to chirality," Phys. Rev. B **79**(3), 035407 (2009).
[5] S. Zhang, Y.-S. Park, Jensen Li *et al.*, "Negative refractive index in chiral metamaterials," Phys. Rev. Lett. **102**(2), 023901 (2009).
[6] J. Zhou, J. Dong, B. Wang *et al.*, "Negative refractive index due to chirality," Phys. Rev. B **79**(12), 121104(R) (2009).
[7] X. Xiong, W.-H. Sun, Y.-J. Bao *et al.*, "Construction of a chiral metamaterial with a U-shaped resonator assembly," Phys. Rev. B **81**(7), 075119 (2010).
[8] M. Decker, M. W. Klein, M. Wegener *et al.*, "Circular dichroism of planar chiral magnetic metamaterials," Opt. Lett. **32**(7), 856–858 (2007).
[9] M. Decker, M. Ruther, C. E. Kriegler *et al.*, "Strong optical activity from twisted-cross photonic metamaterials," Opt. Lett. **34**(16), 2501–2503 (2009).
[10] M. Decker, R. Zhao, C. M. Soukoulis *et al.*, "Twisted split-ring-resonator photonic metamaterial with huge optical activity," Opt. Lett. **35**(10), 1593–1595 (2010).
[11] Y. Svirko, N. Zheludev, and M. Osipov, "Layered chiral metallic microstructures with inductive coupling," Appl. Phys. Lett. **78**(4), 498–500 (2001).
[12] A. V. Rogacheva, V. A. Fedotov, A. S. Schwanecke *et al.*, "Giant gyrotropy due to electromagnetic-field coupling in a bilayered chiral structure," Phys. Rev. Lett. **97**(17), 177401 (2006).
[13] E. Plum, V. A. Fedotov, A. S. Schwanecke *et al.*, "Giant optical gyrotropy due to electromagnetic coupling," Appl. Phys. Lett. **90**(22), 223113 (2007).
[14] A. V. Krasavin, A. S. Schwanecke, and N. I. Zheludev, "Extraordinary properties of light transmission through a small chiral hole in a metallic screen," J. Opt. A, Pure Appl. Opt. **8**(4), S98 (2006).
[15] T. J. Sluckin, "The liquid crystal phases: Physics and technology," Contemp. Phys. **41**(1), 37–56 (2000).
[16] C. Croenne, F. Garet, E. Lheurette *et al.*, "Left handed dispersion of a stack of subwavelength hole metal arrays at terahertz frequencies," Appl. Phys. Lett. **94**(13), 133112 (2009).
[17] S. Wang, F. Garet, K. Blary *et al.*, "Composite left/right-handed stacked hole arrays at submillimeter wavelengths," J. Appl. Phys. **107**(7), 074510 (2010).
[18] S. Wang, F. Garet, K. Blary *et al.*, "Experimental verification of negative refraction for a wedge-type negative index metamaterial operating at terahertz," Appl. Phys. Lett. **97**(18), 181902 (2010).
[19] J. Carbonell, C. Croenne, F. Garet *et al.*, "Lumped elements circuit of terahertz fishnet-like arrays with composite dispersion," J. Appl. Phys. **108**(1), 014907 (2010).
[20] F. Garet, L. Duvillaret, and J.-L. Coutaz, "Evidence of frequency-dependent THz beam polarization in time-domain spectroscopy," Proc. SPIE **3617**, 30–37 (1999).